Partial Discharge Testing of Solder Fillets on PCBs in a Partial Vacuum: New Experimental Results

Lorenzo Capineri, *Member, IEEE*, Gabriele Dainelli, Maurizio Materassi, and Barrie D. Dunn

***Abstract*—This work investigates the influence on the partial discharge (PD) onset due to the geometry of solder fillets of aerospace and spacecraft component assemblies operating in vacuum and at high voltages.**

An automatic measuring system has been developed and calibrated to detect PD signals in vacuum (proportional to the apparent charge) which are recorded and displayed in terms of amplitude and temporal distributions. The experimental part of the project is aimed at investigating the influence of the geometry of solder fillets (produced according to the European space industry standard, ECSS-Q-70-08), on the occurrence of PD activity. Stranded terminals of high voltage cables were soldered to circular copper pads on FR4 fiberglass epoxy printed circuit board (PCB). Various copper electrode configurations have been produced and, prior to the test program, they were characterized for dimensional, electrical and optical properties. Two types of solder fillet geometries have been realized for each electrode configuration: round joints with an abundance of solder and sharp pointed joints made with minimal solder. The minimum distance between electrodes for all samples is nominally 5 mm. Paschen-like curves were established from measurements performed where the product of *pressure x distance* lies in the range of 2 mbar mm–50 mbar mm. Corona inception voltage (CIV) and corona extinction voltage (CEV) values were recorded at different values of *pressure x distance*. Stable glow discharge triggering voltage and current were also measured. The experimental results indicated that the PD activity for the sharp pointed pads and sharp pointed joints is greater than the other cases, but no significant differences (less than 50 V) of the values of CIV and CEV have been found.

***Index Terms*—High voltage systems, partial discharges, printed circuit board, solder fillets.**

I. Introduction

A STUDY of the partial discharge (PD) phenomenon, which occurs when electronic circuits and equipments operate at low pressure and high voltages, is of great interest to electronic engineers and product assurance personnel. The study relates mainly to avionics and spacecraft electrical assemblies. In space electronics the increasing number of electrical and electronic devices operating at high voltages (HV), in particular dc power supply, has prompted new technological research and new testing methods to improve the reliability of HV systems during service. Some examples of these devices working at high dc voltage (HVDC) on satellites are as follows.

Manuscript received February 1, 2003; revised August 25, 2003. This work was supported by the Italian Space Agency under Research Contract ASI I/R/142/01.

L. Capineri is with the Dipartimento Elettronica e Telecomunicazioni, Università di Firenze, Firenze 50131, Italy (e-mail: capineri@ieee.org).

G. Dainelli and M. Materassi are with the Laben-Proel Tecnologie Division, Università di Firenze, Firenze 50131, Italy.

B. D. Dunn is with the ESA-ESTEC, Noordwijk, The Netherlands.

Digital Object Identifier 10.1109/TEPM.2003.820822

- Ionic propulsion systems.
- Photomultiplier tubes (PMT).
- Scientific electronic instruments.
- Radar or communication systems using Travelling Wave Tubes (TWT).
- Solar cell power supply systems.

For HV components operating in a space environment there are several factors that can increase the potential failure of such devices [1] and a method to ensure proper insulation characteristics is to exploit the space vacuum. This is a good solution but in accordance with Paschen's law, a designer must consider the problem of a variable *pressure x distance* product (Pd) during the life of the spacecraft. In this case the Pd range includes the minimum electric field strength at which a glow discharge starts for a two-electrode system in a gas. This variation of Pd has been demonstrated in some cases to be sufficient for PD onset in electronic systems even at voltages of 400 V to 1000 V, even though these voltage values are not critical for the electronics operating at ambient pressure on earth (760 mbar) or at low pressure (typically 10^{-5} bar) corresponding to the spacecraft's final orbit.

The investigation of the PD phenomenon helps the designer of aerospace electronic systems to adopt criteria capable of reducing the aging, acoustic noise, energy waste and the probability of failure. Most space apparatus are only electronically activated once they have reached a position in final orbit. Generally spacecrafts are left nonoperational for two or three days allowing outgassing until a stable and very low pressure is reached. If HV equipment were to be switched on during this intermediate period, critical pressures caused by spacecraft venting and outgassing would certainly cause problems related to PD. When well known design rules such as the selection of low outgassing materials, increased insulation thickness, use of defect-free dielectric materials and, finally, worst case analysis of electric field stress in the HV devices [2], [3] PD phenomena can often be avoided or ignored.

The present work addresses the problem of PD phenomena induced by stranded terminals of HV cables soldered to copper pads on FR4 fiberglass PCB. A previous study [4] aimed to investigate the influence of solder fillet geometry on PD activity. Insulated terminals were soldered to a pair of symmetrical copper pads on printed circuit boards. The soldered joints conformed to the European Space workmanship standard document ECSS-Q-70-08. That study consisted of an experimental set-up for carrying out testing on a variety of samples located in a vacuum chamber. The aim was to verify that the sharp geometry of a solder fillet can increase the electric field stress and consequently the PD activity with respect to another possible geometry with a rounded shape and abundant solder (these are, respectively, rejectable and acceptable HV soldered

joints according to the design rules of the ECSS specification). Both geometries can be space qualified for their mechanical and electrical characteristics, but it was previously thought that the sharp one was more prone to induce PD phenomena at lower voltages and consequently a round shape solder fillet would be preferable from a quality control point of view. Reworking a solder fillet with sharp geometry is possible but because it is time consuming, expensive, and can physically damage the circuit board, it is important to assess the real importance of this problem. The results obtained from that early study were interesting but nonconclusive. Symmetric copper terminal pads on the PCB were used to compare the two geometric types of solder fillets (round and sharp) and several specimens were produced with various distances between electrodes (distance "d"). The measured PDs were recorded for different values of Pd in the range of 1–50 mbar mm. Although the measurements did not show remarkable differences between the values of CIV due to experimental variance, a reproducible situation was observed with a higher repetition rate and amplitude of PD for the sharp fillet geometry. The experience gained with that study suggested that we repeat those experiments with a new project [5] by developing a new experimental set-up capable of recording quantitatively random PD and by defining carefully the fabrication, handling and testing procedures of samples. Moreover, we aimed to enlarge the investigation by including samples with different geometries (symmetrical and nonsymmetrical) of copper pads and electrodes on the PCB but all with the same minimum distance "d."

The experiments reported in this paper present new results obtained with a better developed set-up which allows more flexibility for different measuring tasks and more repeatable testing conditions. These are essential for the investigation of PD phenomena and they are more statistically significant.

This new set-up has the following characteristics, which are useful for general investigations of PD phenomena on a broad range of aerospace and spacecraft assemblies.

- Automatic acquisition and recording of data. This capability allows off-line data analysisand the extraction of statistical parameters which are useful to characterize PD phenomena at dc voltages [6]–[8].
- Programmable HVDC and pressure P inside the vacuum chamber. Monitoring of the actual voltage and pressure during the experiments to increase the measurements' reproducibility.
- Improved sensitivity with respect to the previous set-up [9]–[10]. A linear regulated power supply with low ripple was used and a passive resonant detector of PD has been located inside the vacuum chamber as close as possible to the test object for reducing electromagnetic interference.
- Analysis and definition of the calibration procedure according to an equivalent circuit model of the measuring system, especially for taking into account the effects of parasitic capacitance.

This experimental set-up has been designed with a modular electronic instrument for system calibration in low-voltage mode and for signal conditioning. The versatility of this instrument concerns the use of test-objects with a wide range of capacitance (1 pF–500 pF), different PD levels and testing voltages.

The paper will describe in Section II the testing criteria for PD measurements and the fabrication of solder fillets on PCB samples, Section III covers the characteristics of the experimental set-up, Section IV describes the testing procedure and Section V the experimental results. Finally comments on the experimental data and conclusions are reported in Section VI.

II. PD Testing Criteria and Fabrication of Solder Fillets on PCB Samples

A. Partial Discharge Testing Criteria

The PD phenomenon is assumed in this work to be generated by a spatially non uniform electric field between two electrodes on a PCB that are connected to a HVDC by wires and placed in a vacuum chamber containing air at controlled pressures. During development of this testing procedure it has been necessary to identify and to measure parameters that are useful to show the different behaviors among different electrode geometries of the PD phenomenon deliberately induced in the laboratory. This ensured that a comparative study could be carried out. In the case of HV electrical apparatus operating with an ac power supply, the PD testing can take advantage of the PD phenomena synchronization with the bipolar phases of the electric field within one period. However, in the case of PD tests with dc a more sophisticated measuring system is required to observe, record and analyze PD discharges occurring at random when the applied voltage is sufficiently high to trigger the discharges between electrodes. When a specific voltage value is reached (as explained below) we have far greater visual evidence of the glow discharge associated with the ionization of the gas surrounding the electrodes. There are two characteristic parameters, "CIV" and "CEV," that are commonly used to rate the electric field intensity associated with the first glow discharge visual observation (inception) and its termination (extinction). Both parameters are generally reported as a function of the Pd product according to the empirical Paschen's Law adapted to a specific gas and electrode geometry. Based on our laboratory experiences we decide to use several parameters to discriminate the PD activity of different solder fillet geometries on different PCB samples.

1) Corona inception voltage (CIV): this value indicates the start of the glow discharge for a given electrode geometry and pressure. The measured CIV as function of Pd product provides the *Paschen* curve.
2) Corona extinction voltage (CEV): the value at which the glow discharge is extinguished. It is always less than CIV.
3) I_{glow}: the average current absorbed from the HVDC power supply during the glow discharge regime. This current is not typical during PD phenomena but is rather constant during glow discharge.
4) Discharge amplitude (pk-pk value of the signal envelope): this parameter can be observed directly with an oscilloscope connected to the output of the detection instrument or recorded by the data acquisition board.
5) Visual inspection: from this type of investigation some information can be obtained about the position, color, shape and dimensions of the *glow* and about the localization of arcs between electrodes.
6) Temporal and Amplitude histograms of PD recorded at voltage values lower than CIV.

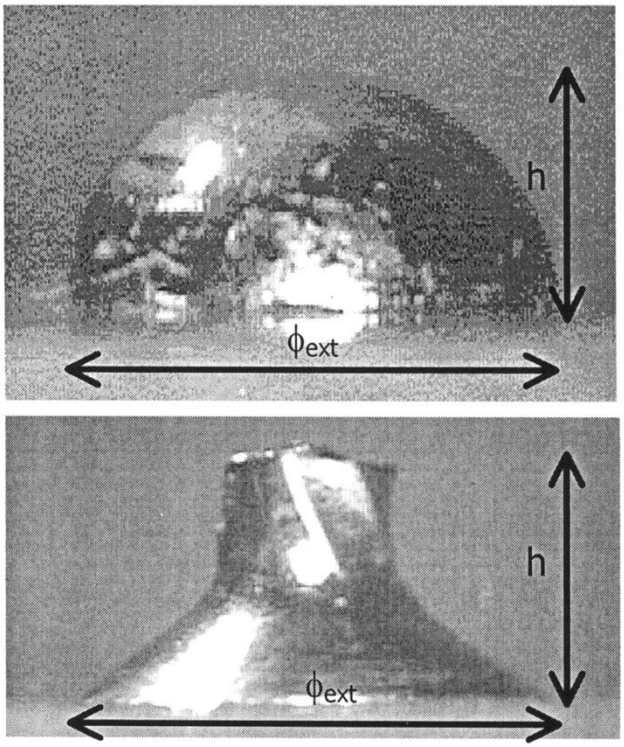

Fig. 1. Detail image of an abundant round shape solder joint (top) and a sharp conic shape solder joint having minimal solder fillet (bottom). The circular copper pads have a $\phi_{\rm ext} = 2.4$ mm. The height h of the solder joints satisfies the reference standard ECSS-Q-70-08 that is (1.5 ± 0.8) mm.

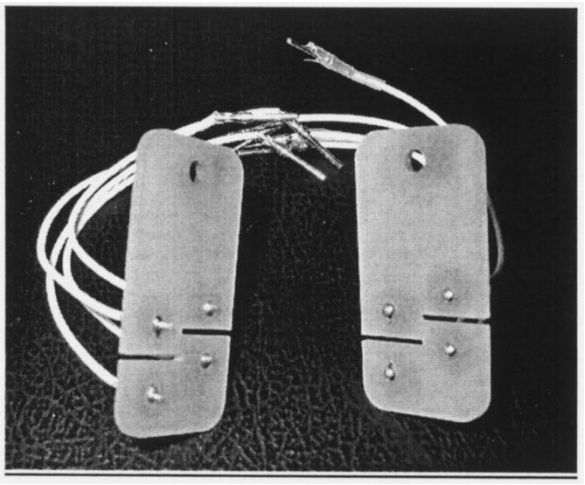

Fig. 2. Example of the two types of solder fillet geometries realized on PCB: (right) sample round abundant shape (RAS) and (left) pointed shape solder (PSS). On each sample there are two type of copper pads: circular and sharp shaped. For the latter, sharpness was obtained by designing the pads with a triangular arrow tip with angle about 57°. The dark colored areas surrounding the soldered terminals are the positions of epoxy that is used to "pot" the wires and cover the insulation clearance on the wire side of the PCB.

B. Fabrication of Solder Fillets on PCB Samples

The copper terminal pads on PCBs were of a simple geometry. Each pad is insulated, both by the glass-epoxy FR4 PCB substrate and by the surrounding air. It is assumed that there are no defects within the FR4 laminate so that any PD will occur only in the gas contained in the vacuum chamber (at any specified pressure P and temperature). Because the values of CIV and CEV are mainly influenced by the minimum distance between

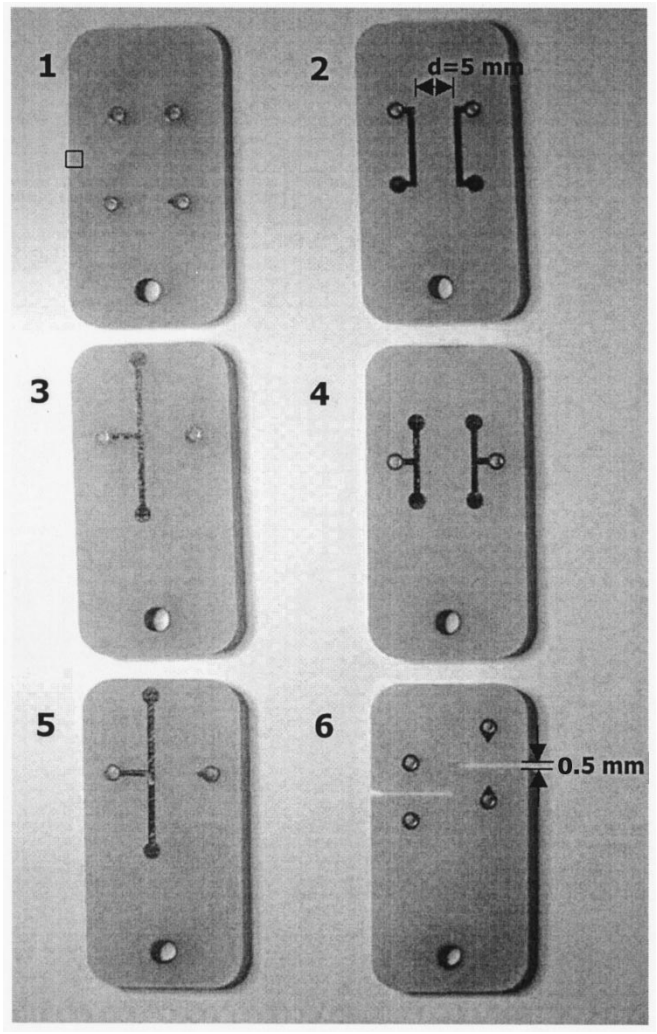

Fig. 3. Six PCB samples with eight different copper pair electrodes all at distance $\mathrm{d} = 5$ mm: (1) two pairs of circular copper pads; (2) pair of parallel lines; (3) a line and a circular pad; (4) two pairs of circular pads connected by parallel lines; (5) a pair of circular pads connected with a line and a sharp pointed pad; and (6) two pairs of circular and sharp pointed pads separated by a 0.5 mm gap on the PCB. Rectangular PCBs are made of space qualified FR4 with dimensions 40 mm × 20 mm × 1.6 mm.

electrodes we set a nominal value $\mathrm{d} = 5$ mm for all samples. This constant distance enabled the results of PD measurements to be easily compared.

Two types of solder fillet geometries are considered: a round shaped type with no protrusions and a stud joint having a sharp profile (see Fig. 1). An operator trained and certified to space quality standards soldered all joints together with tin-lead eutectic. Cleaning used a rosin-based flux. The electrodes were connected to the HVDC power supply by means of a pair of wire terminals (Fig. 2).

These two types of solder joints have been reproduced on eight different electrode configurations in order to test different copper patterns on PCB (see Fig. 3): circular copper pads, pointed shaped copper pads, circular copper pads separated by a 0.5 mm gap on the PCB, pointed shaped copper pads separated by a gap on the PCB, two parallel copper lines, two pairs of copper pads connected by parallel copper lines, one copper line and a circular copper pad, and one copper line and a point shaped copper pad. Certain geometries are duplicated

TABLE I
CHARACTERISTICS OF THE PCB SAMPLES

Type of PCB Sample # (See Figure 3)	Copper pads geometry	Electrical Capacitance C_T[pF]	Minimum distance d [mm]	Type of solder fillets
1 (top)	Pair of circular pads	0.3	4.96	RAS
1 (bottom)	Pair of sharp pads	0.3	5.18	RAS
2	Parallel lines	0.7	4.99	RAS
3	Line and a circular pad	0.2	4.95	RAS
1 (top)	Pair of circular pads	0.5	4.99	PSS
1 (bottom)	Pair of sharp pads	0.2	5.18	PSS
2	Parallel lines	0.3	5.03	PSS
3	Line and a circular pad	0.1	5.1	PSS

on the same PCB in order to have very similar experimental conditions for different solder fillets. This leads to a total of six different PCB designs as shown in Fig. 3.

The influence of copper pad geometries on PD can be compared to the well known traditional three-dimensional experiments with needle-plane, plane-plane and sphere-plane electrodes.

For our investigation PCB samples were manufactured with solder fillets according to a space company standard [11]. The external dimensions of the PCB made of standard FR4 laminate are 40 mm $\times$ 20 mm $\times$ 1.6 mm. The measured average thickness of the copper layer is 26.1 μm (standard deviation 0.8 μm). As mentioned before, the eight electrode configurations have the same separation distance equal to 5 mm. For simplicity we have made the following designations for a total of 18 samples considered for our tests.

- RAS—Round shape and abundant solder.
- PSS—Pointed shape solder with minimal solder

The reference standard for manual soldering is reported in [12]. Examples of the fabricated PCBs are shown in Fig. 2; the cable's length is 8 cm and terminated with Cannon type connector pins. The Gore cable's characteristics are: silver-plated copper, AWG 20, stranded wires (19 $\times$ AWG 32), insulation material PTFE.

Table I summarizes the actual measured solder joint dimensions on samples that were photographed in Fig. 3. This characterization was made for 8 out of 18 fabricated PCB samples and the parameters reported in Table I are: electrode geometry, electrical capacitance C_T including the soldered wires, electrodes minimum distance d and type of solder fillet geometry.

These data show that the nominal minimum distance $d = 5$ mm is reproducible within 2% and the electrical capacitance is always less than 0.7 pF. The heights of the solder joints accomplish the reference standard ECSS-Q-70-08 that is (1.5 ± 0.8) mm. In the case of RAS, the section of the solder shape is a semicircle with base equal to $\phi_{ext} = 2.4$ mm of the circular pad and the corresponding height equal to $\phi_{ext}/2 = 1.2$ mm. In both cases the tolerances of the heights do not affect the CIV that remains determined by the minimum distance and the solder fillet geometry.

In order to ensure that the 18 soldered assemblies retained their material characteristics during the entire test program, they were specially stored in a clean pressurized case.

III. EXPERIMENTAL SET-UP FOR PD DETECTION

A complete system for the detection of a partial discharge in high voltage devices for aerospace applications has been developed according to the guidelines of the IEC 270 standard [13]. This "measurement facility" has characteristics suited for research and technological investigations on electronic devices for components for aerospace and spacecraft applications as the samples can be placed in a glass vacuum chamber with controlled pressure. The measurement system comprises the following items.

1) High Voltage (0–20 kV) programmable dc Power Supply with linear regulator.
2) Vacuum chamber.
3) Turbo-molecular vacuum pump, programmable (10^{-2} mbar–10 mbar).
4) Partial discharge resonant detector inside the vacuum chamber with a passive bandpass filter (30 kHz–200 kHz @-3 dB).
5) Partial discharge calibration and signal conditioning instrument.
6) Software for real-time partial discharge acquisition/processing developed in LabVIEW, with a data acquisition board 12 bit/1.25 MHz (Model Keithley KPCI3110).

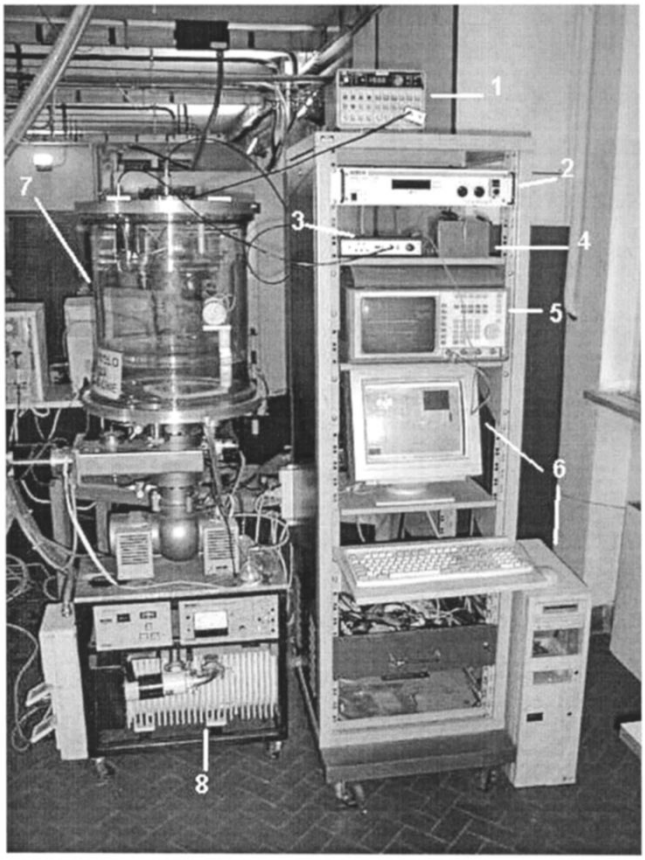

Fig. 4. Experimental set-up with the PD detector in the vacuum chamber and signal processing unit: (1) function generator, (2) high voltage (0–20 kV) programmable dc power supply, (3) PD calibration and signal conditioning instrument, (4) battery $\pm 12\ V_{DC}$, (5) digital oscilloscope, (6) personal computer with software for PD Acquisition/Processing in real/time (LabVIEW) for a data acquisition board 12 bit/1.25 MHz, (7) vacuum chamber and PD passive detector, and (8) programmable turbo molecular vacuum pump in the range 10^{-2} mbar to 10 mbar.

All these components are shown in the experimental set-up Fig. 4.

The block scheme of the whole PD measurement system is shown in Fig. 5(a).

The electric circuit of the passive PD detector is shown in Fig. 5(B) with the test object capacitance C_T and the programmable HV negative power supply.

A. Component Placement in the Vacuum Chamber

The vacuum chamber is a thick glass cylinder (diameter 45 cm, height 50 cm), and the removable aluminum top is provided with feed-through for electrical connections. A rubber washer ensures the seal between the aluminum and the glass. The passive detector, the coupling capacitance, the ballast resistor for the dc power supply and the plastic PVC holder for the test objects and cables are placed inside the vacuum chamber (see Fig. 6).

B. Calibration of the PD Detector

The system provides quantitative measurements of PD by the output voltage signals from the resonant detector. The voltage

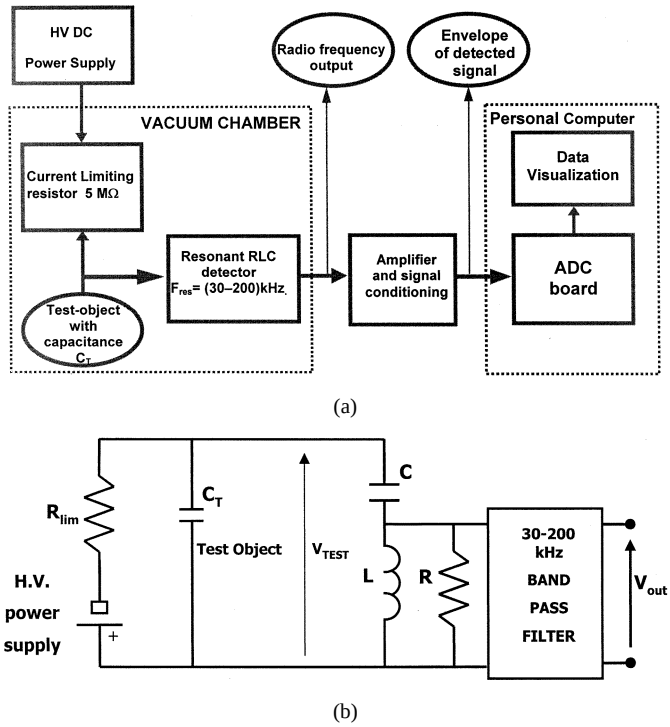

Fig. 5. (a) Block diagram of the system for PD testing in vacuum and data analysis. (b) Electrical circuit of the passive resonant partial discharge detector and bandpass filter both placed in the vacuum chamber.

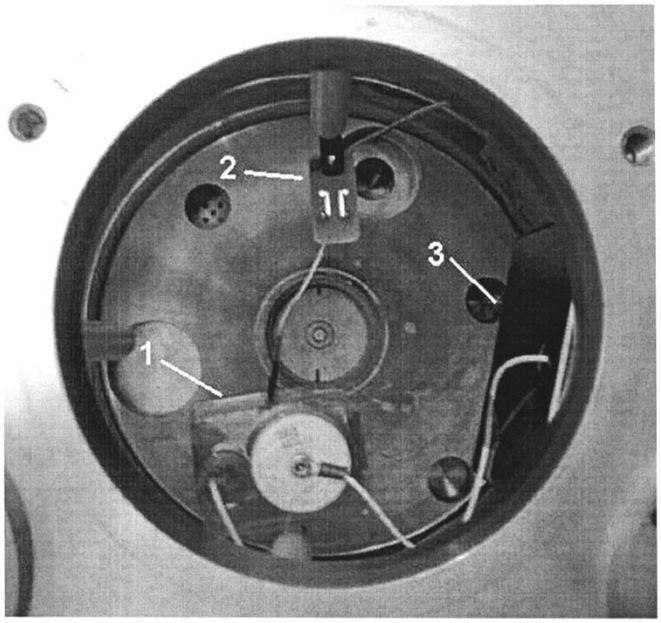

Fig. 6. Top view of the vacuum chamber (aluminum top removed). The figure shows the main components described above: (1) Coupling capacitance and limiting resistor potted in the same resin block; (2) PCB sample under test; (3) Passive resonant PD detector.

amplitude corresponds to an apparent charge[1] after system calibration. The system calibration was carried out using an electronic instrument [14] where current pulses with different levels, repetition frequency and calibration capacitance can be varied

[1]Apparent charge definition: it produces the same effects on the terminals' voltage as the charge actually involved locally at the side of the PD during transient.

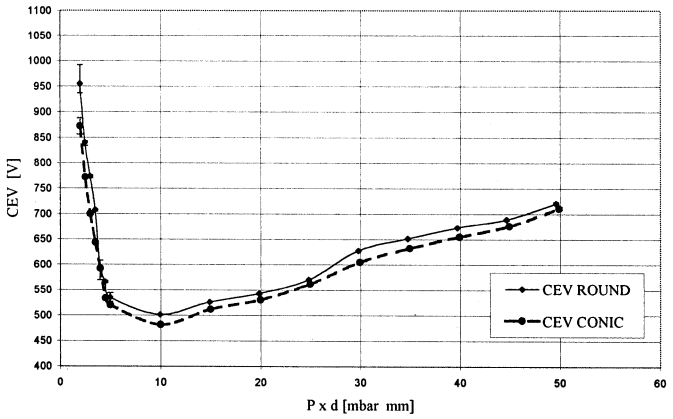

(a)

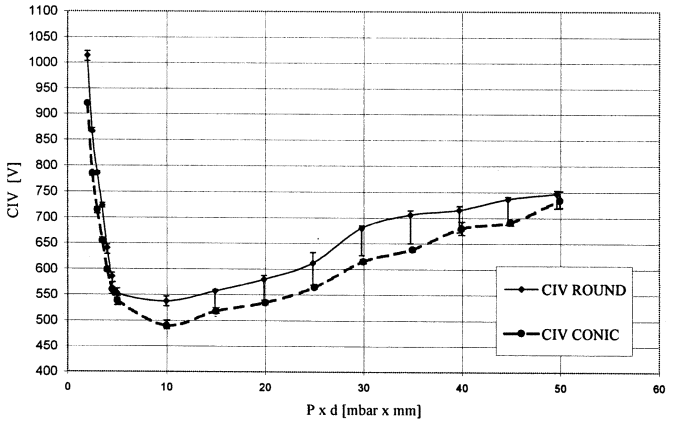

(b)

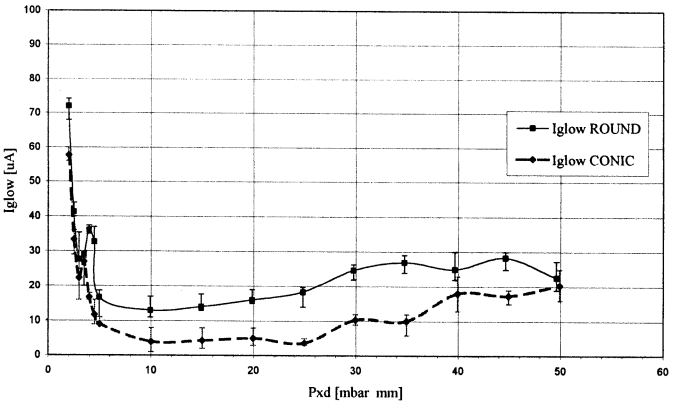

(c)

Fig. 7. Case 1: Pair of circular pads: (a) CEV, (b) CIV, and (c) I_{glow}.

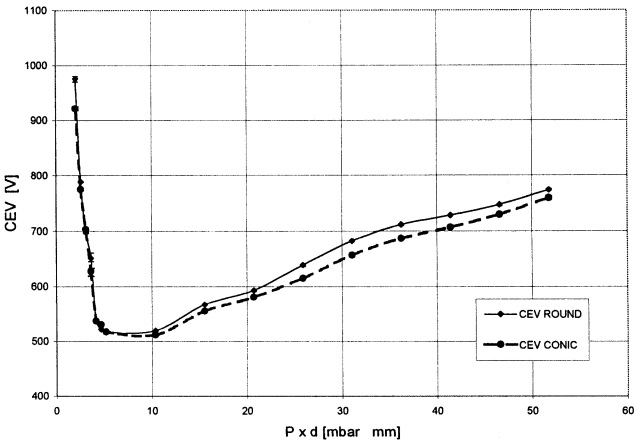

(a)

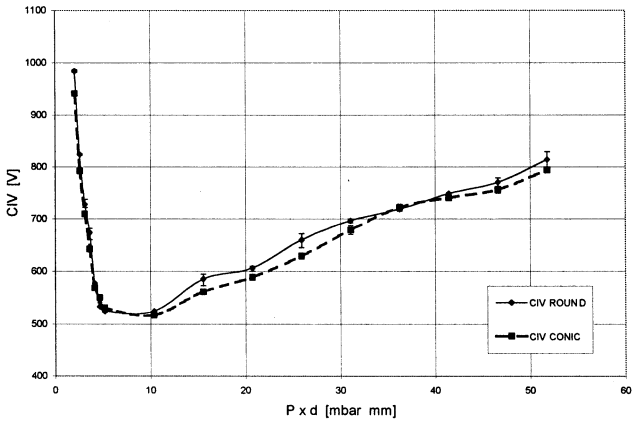

(b)

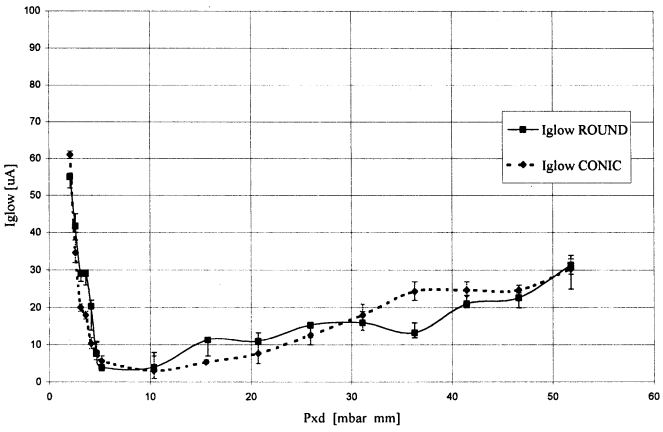

(c)

Fig. 8. Case 2: Sharp pads: (a) CEV, (b) CIV, and (c) I_{glow}.

in suitable ranges. The output voltages from the detector were measured and compared with those obtained from an equivalent circuit model of the system. The latter were exploited to derive the actual charge transferred into the detector, considering the effects of parasitic capacitance of the connection cables and set-up. After several refinements of the calibration procedure we obtained the system sensitivity: calibration sensitivity $S_{CAL} = 6.43$ mV/pC. A correction factor for the calibration sensitivity was applied to S_{CAL} considering the low electrical capacitance of the test object that was assumed to be 1 pF, leading to a value of $S_{CAL} = 5.12$ mV/pC. A low background level of noise of 0.5 pC was obtained by utilizing appropriate ground, shields, and selecting a commercial low noise HVDC power supply with a linear regulator (Bertan Model 205B). All these specifications are comparable with other PD measurement systems published in the literature.

C. Electronic Instrument for Signal Acquisition and Processing

The designed instrument is modular and also includes a signal conditioning section. A linear variable gain amplifier (voltage gain $A_V = 2$–1000) with bandwidth 120 kHz and dynamic output voltage 12 V_{pp} has been designed in order to maintain a high level of accuracy of calibration under different experimental conditions.

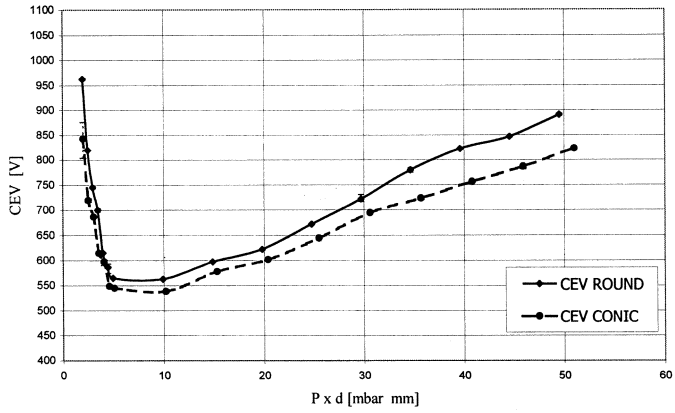

(a)

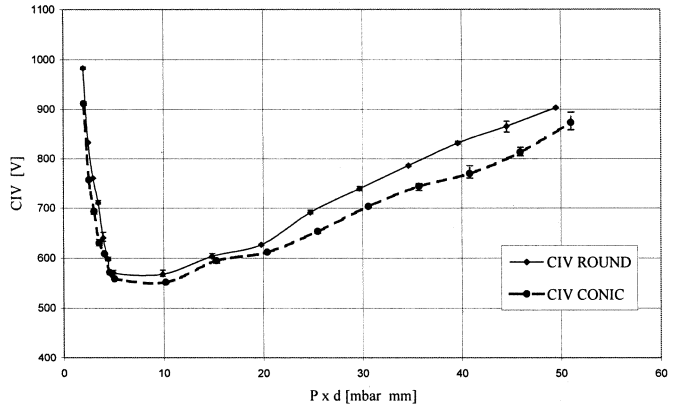

(b)

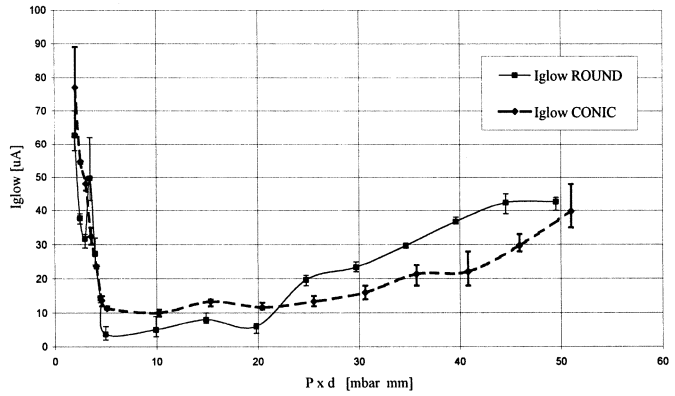

(c)

Fig. 9. Case 3: Circular pad and a line: (a) CEV, (b) CIV, and (c) I_{glow}.

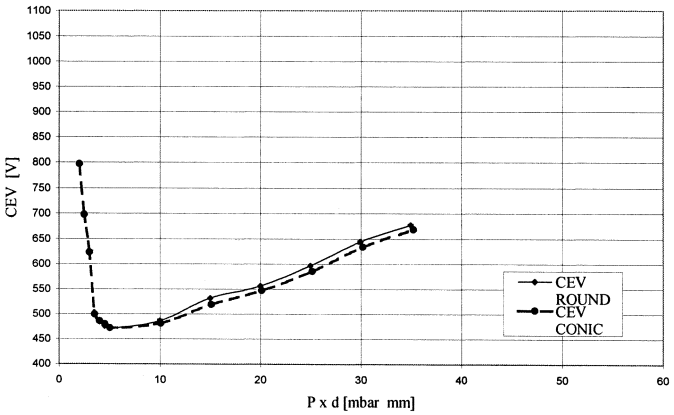

(a)

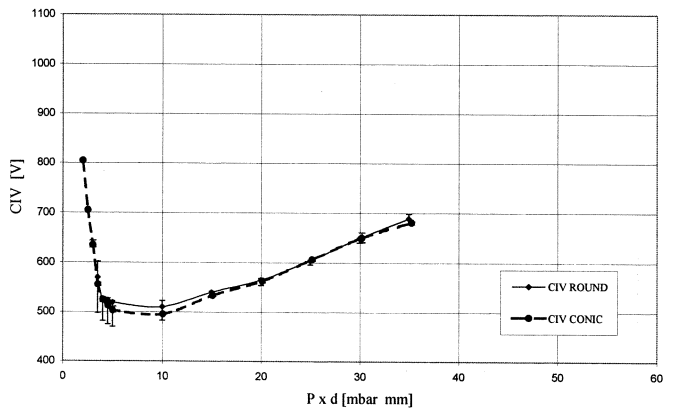

(b)

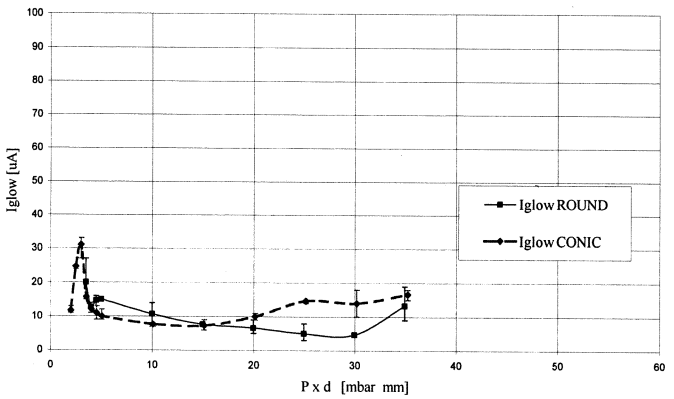

(c)

Fig. 10. Case 4: Parallel lines: (a) CEV, (b) CIV, and (c) I_{glow}.

A series of signal processing programs were developed for the present project. They permit the conditioned signal to be acquired and processed in real-time. The software that was developed shows that the voltage signals corresponding to PD events are greater than a programmable threshold. Amplitude and temporal histograms of the recorded PD events within the measurement interval are shown on the personal computer display as a front panel of a virtual instrument designed with LabVIEW. These two histograms are fundamental for the characterization of PD activity and they can also provide a PD signature of the device under test. The software also allows the temporal profile of the high voltage supply to be defined and this is critical for determining the CIV and CEV values. During measurements, the software controls different parameters: the pressure inside the vacuum chamber, the actual voltage supply on the test sample and the supply current. The monitoring of these parameters has increased the repeatability of the PD tests with respect to our previously reported experiment set-up [4], [10].

IV. Description of the Testing Procedure and Measured Parameters

A testing procedure has been defined by the following steps and then repeated for each single sample.

1) The sample is fixed with the plastic PVC holding system inside the vacuum chamber. The vacuum chamber is cleaned before air purging is started.
2) The vacuum chamber is closed and sealed with the top and the vacuum pump is activated. Evacuation takes place for a specified time.

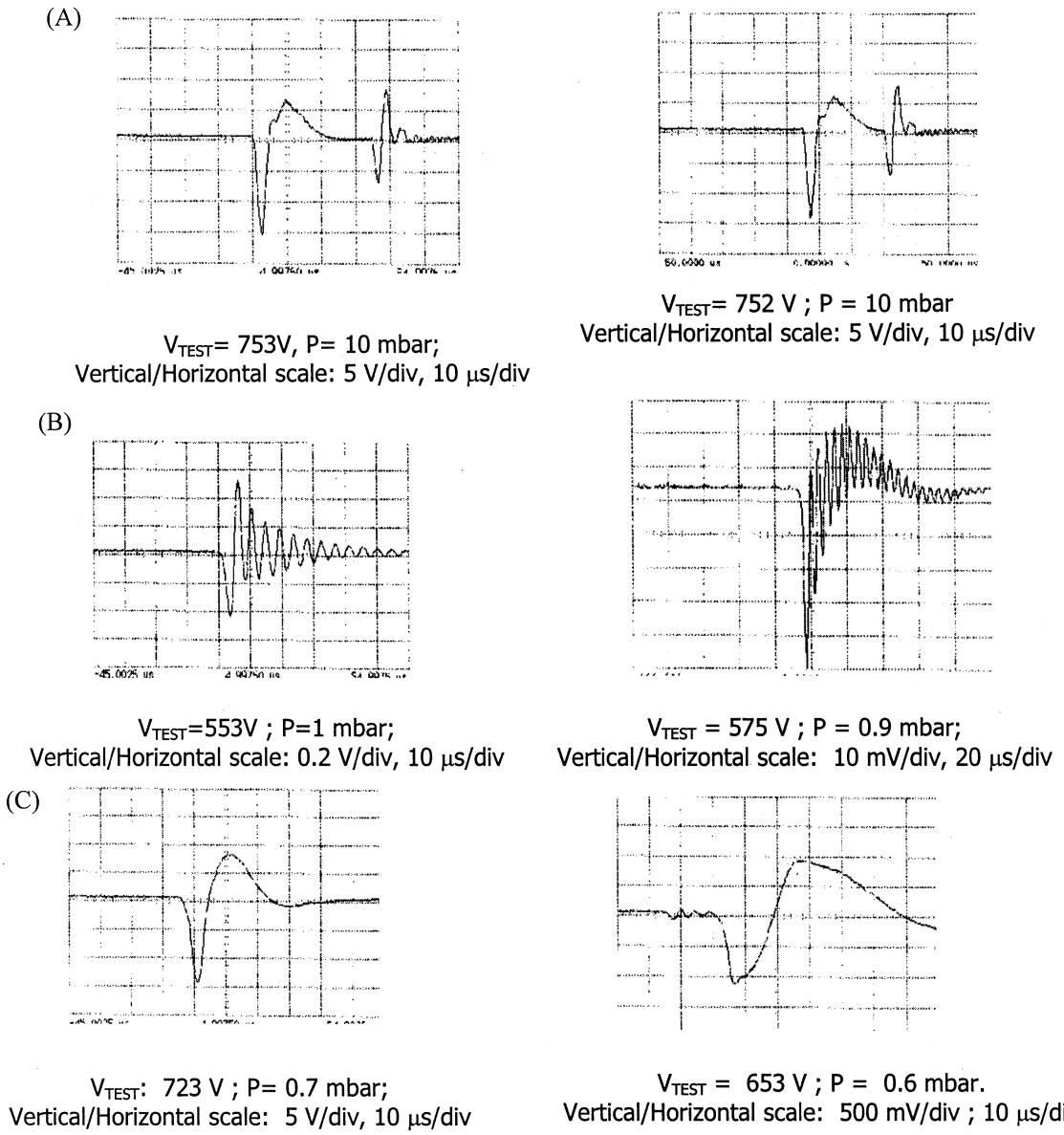

Fig. 11. Typical detected radio frequency signals for a PCB specimen with two circular copper pads at Pd of (a) 50 mbar mm, (b) 5 mbar mm, and (c) 3 mbar mm for two solder fillet geometries: conic (right) and round (left). For each case the test voltage $\mathrm{V_{TEST}}$ (absolute value) is specified.

3) The vacuum inside the chamber is disrupted by introducing air until the final pressure for the test is achieved. The final pressure value is obtained after a settling time of a few minutes.
4) The negative dc testing voltage is obtained by programming the HV power supply and a stepping voltage with 50 V step every 15 s. This is used to set a starting value $\mathrm{V_{START}}$ for the testing at which the glow discharge does not occur.
5) The applied voltage is increased from this value with finer steps and lower slew rate with voltage steps of 1 V every 5 s, until the glow starts. At this time the ramp voltage is stopped and the values of CIV and $\mathrm{I_{glow}}$ are recorded by means of a push button on the virtual panel on the personal computer display. A text area in the front panel of *the* virtual instrument is used to record the visible characteristics of the glow discharge (shape, color, and position).
6) The applied voltage is decreased with the same slew-rate as in the previous step (1 V every 5 s), until the glow extinguishes. Then the CEV value is recorded and the applied voltage is dropped by 100 V from CEV.
7) A relaxation time of 5 min is used before repeating steps 4, 5, 6, 7 of the procedure.
8) The voltage is reset to $\mathrm{V_{START}}$.
9) Steps 3–8 are repeated for all pressure values being considered.
10) The sample is replaced with another one and the procedure repeated from the first step.

In order to relate the experiments to Paschen-like curves the tests are carried out with pressure P in the range (0.3–10) mbar with nominal minimum distance between the pair of electrodes in each sample $\mathrm{d} = 5$ mm. According to this choice the curves will be obtained for a corresponding Pd product in the range 1.5–50 mbar mm.

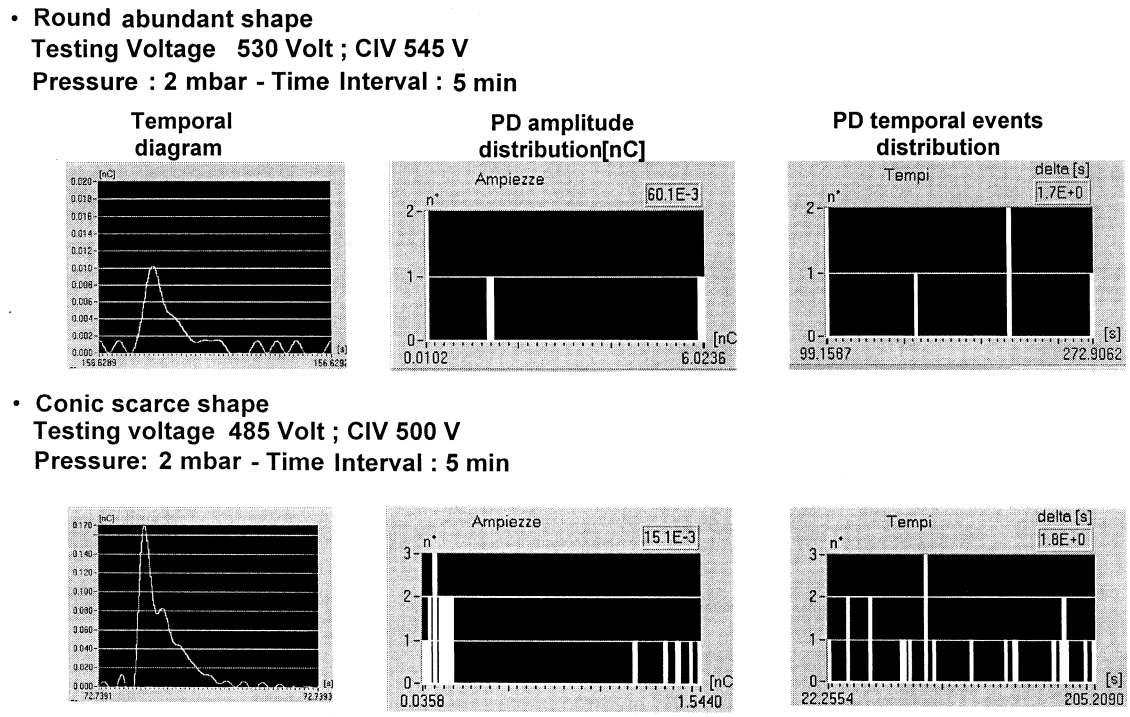

Fig. 12. Amplitude and temporal histograms of PD activity of two solder fillet types before the start of glow discharge. (Top) Round abundant shape geometry. (Bottom) Conic scarce shape geometry.

V. Experimental Results

A first set of results regards the curves relative to the parameters CIV, CEV and I_{glow} that have been measured in several experiments with four electrode geometries and both solder fillet types.

1) Pair of circular pads.
2) Pair of sharp pads.
3) Circular pad and a line.
4) Parallel lines.

In Figs. 7–10 show the curves and the error bands for cases 1–4, with the round geometry indicated by a continuous line and sharp joints by a dashed line.

The following general observations can be reported for each of the four electrode designs.

- During the glow discharge purple colored plasma surrounding the negative electrode can be seen by the naked eye for pressures in the range (0.8–10) mbar. For lower pressures, an intense red color plasma has been observed on the positive electrode. For the single pad and line configuration channeled plasma has been generated between the two electrodes.
- A variation of signal characteristics (amplitude and shape) with pressure is observed in the above temporal diagrams. An example of three signals acquired at Pd values equal to 50, 5, and 3 mbar mm, are shown in Fig. 11(a)–(c) for case 1 with both solder fillet geometries. It has been observed that the signal for the intermediate value of Pd has a ringing characteristic and low amplitude. This is a common feature for cases 1 to 3, where at least one soldered pad was considered, while was not recognized for case 4. Moreover this ringing signal appears in the vicinity of the minimum of the Paschen curves.
- Before the glow discharge occurs at CIV, pure partial discharge phenomena have been recorded. These observations mainly occurred at Pd values around the minimum of the Paschen-like curves.

The latter point suggested more investigations need to be made of the partial discharge activity, acquiring the temporal and amplitude histograms for the two solder fillet geometries. The results reported in Fig. 12 are relative to the case of two symmetrical circular pads. The observation time was 5 min at pressure 2 mbar. In this case the testing voltage was chosen 15 V less than the CIV, that is 530 V and 485 V for the round and conic sharp shapes solder fillets respectively.

Data presented in Figs. 7–10 are also interesting for an understanding of the effects of a reduced pitch between electrodes, which is a goal for designers of compact electronic systems. As expected the behavior of CIV and CEV follow a Paschen like curve and this characteristic confirms the advantages of using a vacuum as an insulator in the low Pd region. Bearing in mind that the minimum distance design criterion is dictated by the maximum operating voltage, there are other considerations for using a vacuum as an insulator. In space applications unexpected failures of pressurized systems or degassing phenomena of components in proximity to high voltage electrodes, can raise the Pd value to around the minimum of the Paschen curve leading to PD activity or even glow discharge initiation.

Minimum pitch also decreases the surface resistance and consequently increases leakage currents. Moreover flux residues due to the soldering process can bridge two solder joints when cleaning is inadequately performed. Careful analysis of these

factors allows the designer to decide between vacuum or solid dielectric insulation systems.

VI. Conclusion

In the light of the experimental results shown in the previous section the following final observations and conclusions can be reported.

i) The improved sensitivity of the present laboratory set-up has confirmed that the corona inception voltage (CIV) of the solder joint configurations having sharp solder fillets have a *Paschen* curve minimum value of 550 V. This is only 50 V lower than the 600 V minimum determined for round, smooth solder joints.

ii) Two electrode geometries with parallel copper lines and facing sharp corner electrodes, with solder terminals at a distance greater than 5 mm, have not revealed substantial differences in terms of PD activity (amplitude and temporal histograms) between the two types of solder fillets. This confirms the theoretical assumptions which predict that it is the minimum distance between electrodes which influences the CIV value and hence the PD activity. This reinforces the design rule that soldered terminals on PCBs should be kept as far apart as possible.

iii) Concerning the curves relative to the glow discharge current I_{glow}, it can be considered that a 5 MΩ ballast resistor was introduced to prevent unexpected current overloads on the HV power supply and to separate the partial discharge resonant circuit from the low internal impedance of the HV power supply. The ballast resistor has prevented a complete characterization of the glow discharge which, according to the literature [15], necessitates of a sustainable current in the order of mA. The variations observed in the I_{glow} curves (ripples and crossovers) are due to the statistical fluctuations of the measured values (10 for each value of P). Future studies will address the characterization of the I_{glow} for different samples without the limitations due to the ballast resistor and/or the maximum current of the HV power supply.

iv) This factor is also important for the insulation and has influence on PD onset. Moreover the presence of residues of flux can bridge two solder joints at minimum distance.

v) These results confirm more quantitatively the hypothesis made in our previous study [4] that the shapes of the solder fillets, whether sharp or rounded, have very little influence on the CIV values. The present European standard [12] recommends that sharp points should be avoided and reworked to become rounded. This activity might damage either the PCB (e.g., pad lifting) or the component (overheating) and our findings indicate that solder connections having protuberances should not be "touched up."

Acknowledgment

The authors would like to thank Prof. L. Masotti, Group Leader of the Ultrasound and Non Destructive Testing Laboratory, University of Florence, Italy, for inspiring this research and for promoting the collaboration with LABEN-PROEL Division, and the Technical Reviewers and Associate Editor Dr. I. Fidan, for their constructive reviews and remarks.

References

[1] P. Rustan, H. Garrett, and M. J. Schor, "High voltages in space: Innovation in space insulation," *IEEE Trans. Elect. Insul.*, vol. 28, pp. 855–865, Oct. 1993.

[2] M. Gollor and K. Rogalla, "HV design of vacuum-insulated power supplies for space applications electrical insulation," *IEEE Trans. on Elect. Insul.*, vol. 28, pp. 667–680, Aug. 1993.

[3] E. Kuffel and W. S. Zaengl, *High Voltage Engineering—Fundamentals*. Oxford, U.K.: Pergamon, 1984.

[4] M. Materassi, B. D. Dunn, and L. Capineri, "The influence of solder fillet geometry on the occurrence of corona discharge during operation between 400 V and 900 V in partial vacuum," *IEEE Trans. Electron. Packag. Manufact.*, vol. 23, pp. 104–115, Apr. 2000.

[5] L. Capineri, "Non destructive testing method of welds for applications in vacuum and high voltage," Final Rep. Italian Space Agency Project Research Contract ASI I/R/142/01, Dept. Electron. Telecommun., Univ. of Florence, Florence, Italy, 2001.

[6] E. Gulski, "Digital analysis of partial discharge," *IEEE Trans. Elect. Insul.*, vol. 2, pp. 822–835, Oct. 1995.

[7] E. Carminati and M. Lazzaroni, "PD detection: A new approach," in *IEEE Instrum. Meas. Technol. Conf.*, St. Paul, MN, May 18–21, 1998.

[8] P. Osvàth, "Comment and discussion on digital processing of PD pulses," *IEEE Trans. Dielectrics. Elect. Insul.*, vol. 2, pp. 685–699, Aug. 1995.

[9] L. Capineri, "Relazione tecnica finale sui metodi e la strumentazione per prove di scariche parziali," Int. Rep. Laben-Proel 30 206, 1993.

[10] S. Pesce, "Metodo di controllo non distruttivo di saldature per applicazioni spaziali basato sul fenomeno di scariche corona: contributo allo sviluppo e verifiche sperimentali," Laurea thesis, Univ. of Florence, Florence, Italy, 1997.

[11] *Master Design for Printed Circuit Boards Production*, LABEN SpA-Operative Instruction IQ-04T-001, Jan. 1997.

[12] *Manual Soldering of High Reliability Electrical Connections*, ECSS-Q-70-08 Space product assurance, 1999.

[13] *Partial Discharge Measurements*, IEC Standard Publication 270, 1981.

[14] G. Dainelli, "Sistema di misura automatico di scariche parziali di oggetti campione in vuoto," Laurea thesis, Univ. of Florence, Florence, Italy, 2000.

[15] J. M. Meek and J. D. Craggs, *Electrical Breakdown of Gases*. Oxford, U.K.: Clarendon, 1953.

Lorenzo Capineri (S'84–M'88) was born in Firenze, Italy, in 1962. He received the Laurea degree in electronic engineering and the Ph.D. degree in non destructive testing from the University of Florence, Italy, in 1988 and 1993, respectively.

Since 1995, he has been a Researcher in electronics with the Department of Electronic Engineering, University of Florence, and now an Associate Professor of electronics. His current research activities are in design of ultrasonic and pyroelectric sensors and related signal processing systems. He was a Visiting Scientist at Harwell and Culham Laboratory, Culham, U.K., working on ground penetrating radar image processing for buried objects detection. He worked in several projects in collaboration with national industries, the Italian Research Council (CNR) and Italian Space Agency (ASI) and European Space Agency (ESA). He is a co-author of four Italian patents on ultrasonic devices.

Gabriele Dainelli was born in Florence, Italy, in 1972. He received the Laurea degree in electronic engineering from the University of Florence, Italy, in 2000.

He joined Laben S.p.A., Florence in the same year and has been employed since then in topics related to electronic design for plasma diagnostic systems.

Maurizio Materassi received the Laurea degree in physics from the University of Florence, Italy, in 1991.

He joined Proel Tecnologie (now incorporated in Laben S.p.A.), Florence, in the same year and has been employed since then in testing activities related to space material and processes. He is currently a Program Manager and is involved in the development of payloads to be flown on board the International Space Station.

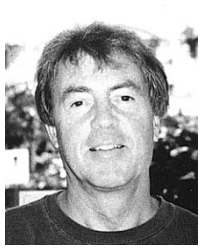

Barrie D. Dunn received the M.Phil degree in metallurgy and the Ph.D. degree in materials technology from Brunel University, U.K., in 1984 and 1986, respectively.

He is currently Head of the Materials and Processes Division, European Space Agency (ESA-Estec), Noordwijk, The Netherlands. He has supported all ESA space projects, particularly the telecommunication satellites and the manned Spacelab and Columbus International Space Station element. He provides expertise on spacecraft assembly processes to INTELSAT, INMARSAT, and national space organizations and is author of the book *Metallurgical Assessment of Spacecraft Parts, Materials and Processes* (Chichester, U.K.: Praxis Publishing, 1997).